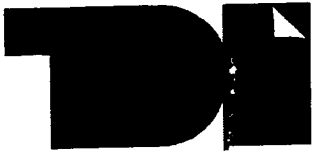


7C02243



TDI LIBRARY SERVICES

11340
Olympic Blvd.
Suite 355
Los Angeles
California
90064-1639
P (310) 268-0601
F (310) 268-0701
tdi@tdico.com

BILL TO

Ut-Battelle
Bldg. 4500N, MS-6193
PO Box 2008
Oak Ridge, TN 37831-6193
USA

SHIP TO

James Kidder
Ut-Battelle

Date Rec'd

03/02/2007

Need By

[Empty box]

Ordered By

[Empty box]

P (865) 574-1241

F (865) 574-1240

Requestor

James Kidder

Client Number

52715X

Service & Delivery

REGULAR FedEx

Journal/Book Title

Canadian Journal of Remote Sensing

Author 1

Latifovic R

Author 2

Pouliot D

Month	Year	Volume	Issue	Pages
	2005	31		347-63

Article Title

Multitemporal land cover mapping for Canada: methodology and products

Order Special Instructions

MC: 4500N 6191

Further reproduction may be a violation of copyright law

Multitemporal land cover mapping for Canada: methodology and products

Rasim Latifovic and Darren Pouliot

Abstract. A mapping methodology is presented for generating a land cover time series from coarse spatial resolution earth observation data. Historically, this has been a difficult task because of inconsistencies that can arise between maps due to inherent noise present in satellite observations. The new methodology reduces the inconsistency by incorporating several information sources unique to the presented approach of updating an existing land cover map backward and forward in time. It consists of change detection and a local evidence classification decision rule that incorporates the local spectral similarity for each class, local land cover proportions, and expected class changes based on the previous class and change direction. The methodology has been implemented to produce land cover maps of Canada for 1985, 1990, 1995, and 2000 from data acquired by the series of National Oceanic and Atmospheric Administration (NOAA) – advanced high-resolution radiometer (AVHRR) sensors. Accuracy assessment based on medium-resolution (30 m) reference data shows that land cover data produced with this new approach have an overall accuracy similar to that of other 1 km resolution land cover maps of Canada, but this product maintains high consistency between years, with a thematic resolution of 12 classes. An analysis of spatial and temporal patterns of land cover disturbances demonstrates the potential application of the multitemporal land cover time series.

Résumé. On présente une méthodologie de cartographie pour la génération d'une série chronologique du couvert à partir de données d'observation de la Terre à résolution spatiale grossière. Traditionnellement, ceci a toujours constitué une tâche difficile à cause des incohérences qui peuvent se manifester entre les cartes dues au bruit inhérent présent dans les observations satellitaires. La nouvelle méthodologie réduit cette incohérence en incorporant plusieurs sources d'information uniques à l'approche présentée de mise à jour d'une carte existante du couvert antérieurement et postérieurement dans le temps. Celle-ci repose sur la détection du changement et une classification basée sur l'évidence locale utilisant une règle de décision qui incorpore la similarité spectrale locale pour chaque classe, les proportions locales du couvert et les changements de classe anticipés basés sur la classe précédente et la direction du changement. La méthodologie a été implantée pour produire des cartes du couvert du Canada pour 1985, 1990, 1995 et 2000, à partir des données acquises par la série de capteurs AVHRR de NOAA. L'évaluation de la précision basée sur des données de référence à résolution moyenne (30 m) montre que les données du couvert produites à l'aide de cette nouvelle approche ont une précision globale similaire à celle des autres cartes du couvert du Canada à une résolution de 1 km, mais ce produit conserve une cohérence élevée au cours des années avec une résolution thématique de 12 classes. Une analyse des patrons spatiaux et temporels des perturbations du couvert démontre le potentiel d'application des séries chronologiques multi-temporelles du couvert.

[Traduit par la Rédaction]

Introduction

Long-term observations of the earth system sustained over decades are a critical first step for providing the information necessary for scientists, decision makers, and stakeholders to assess human impacts and vulnerability associated with environmental change. Among the most important environmental parameters that summarize the physical, biotic, and climatic components of terrestrial ecosystems are distributions of vegetation, water, snow and ice, and other land cover types. These land surface characteristics are needed for parameterization of climatic, ecological, and natural resources applications at global and regional scales.

The current approach to defining surface parameters at the regional scale in the absence of field-derived parameters is to use coarse-resolution satellite data as a primary source of information. Mapping vegetation and land cover on a yearly basis at regional and global scales using remotely sensed data has a rich history of application. The first regional product, a land cover map of Africa, based on National Oceanic and

Atmospheric Administration (NOAA) – advanced high-resolution radiometer (AVHRR) data was produced by Tucker et al. (1984). Subsequently, Townshend et al. (1987) created a map of South America, Cihlar et al. (1999) created a map for Canada, and global land cover maps were produced by Loveland and Belward (1997; for the International Geosphere–Biosphere Programme (IGBP)), DeFries and Townshend (1994), and Hansen et al. (2003). More recent global maps have been produced from SPOT VEGETATION data (Latifovic et al., 2004) and moderate resolution image spectroradiometer

Received 15 December 2004. Accepted 20 May 2005.

R. Latifovic.¹ Canada Centre for Remote Sensing, Natural Resources Canada, 588 Booth Street, Ottawa, ON K1A 0Y7, Canada.

D. Pouliot. Noetix Research Inc., 588 Booth Street, Ottawa, ON K1A 0Y7, Canada.

¹Corresponding author (e-mail: Rasim.Latifovic@CCRS.NRC.gc.ca).

(MODIS) data (Strahler et al., 1999). Nonetheless, there have been few attempts at producing a long-term land cover time series of sufficient length, consistency, and continuity for studying patterns of environmental variability and change. This is a difficult task due to noise present in long-term satellite data acquired over large areas with 1 km spatial resolution. There are many reasons for inconsistency in long-term satellite data; some of them are because of differences in atmospheric conditions (aerosol, haze, and water vapor content) and acquisition geometry (bidirectional effects, geometric misregistration, and variable ground pixel size) (Cihlar et al., 2004), and others are in relation to vegetation phenology (Stöckli and Vidale, 2004), sensor-related noise, cross-sensors calibration (Trishchenko et al., 2001), and drift in equatorial crossing time.

Standard procedures for temporal land cover evaluation have employed change detection analysis based on different techniques including image differencing, principal component analysis, and postclassification comparison. Recent developments in this area have utilized spectral mixture analysis, artificial neural networks, and integration of geographic information systems (GIS) and remote sensing data. Comprehensive overviews of change detection techniques are presented in Coppin et al. (2004) and Lu et al. (2004). To be successful, a change detection analysis requires, as a prerequisite, multitemporal image registration, radiometric and atmospheric correction, or normalization between images at the same spatial and spectral resolution (Coppin and Bauer, 1996; Jensen, 1996). Data preprocessing is a crucial part of change detection analysis because the level of achievable change detection accuracy will depend, to a large extent, on the degree to which these prerequisites are met.

Multitemporal comparison between classified maps requires high accuracy that is difficult to achieve with coarse-resolution data. Maxwell et al. (2002a; 2002b) produced a land cover time series (1990–1995) for the state of Colorado from AVHRR data following a supervised classification approach. The average overall accuracy of these maps was good (~82%), but the error for postclassification change detection could range from 0% to 38% depending on the nature of the errors in the individual maps. It is difficult to determine the exact magnitude, but it is widely recognized that the accuracy of postclassification change detection is approximately the product of the two input classification accuracies (Coppin et al., 2004). For the aforementioned case, change detection accuracy would be ~67%. In addition to the potential for very large error, this approach is also very labor intensive, requiring a substantial amount of time and expertise to create the classified products.

The MODIS global land cover product is another example of a land cover time series. It employs the latest technology in sensor development, calibration, and processing techniques. However, it does not extend sufficiently far back in time for meaningful temporal analysis, and rigorous validation of products is still pending. In moderate-resolution data (e.g., Landsat), there are numerous examples of the post-detection

classification approach (Hall et al., 1991; Miller et al., 1998; Mas, 1999; Foody, 2001; Latifovic et al., 2005).

Although typically performed separately, land cover mapping and change detection are techniques that are highly complementary for the objective of multitemporal land cover mapping. The method we present in this paper consists of two main steps: (i) change detection with an existing land cover map, and (ii) classification of these changes to create an updated land cover product. The updates can be applied periodically to the baseline land cover product to extend the temporal dimension of the land cover time series.

The objective of this study was to develop a methodology to produce a consistent land cover time series at a regional scale that can be used for tracking environmental changes resulting from human and natural disturbances. Here, consistency refers to the overall agreement between two land cover maps and should not be lower than the expected amount of change that an area would expect to experience over a selected time interval. The specific objectives were as follows: (i) develop a multitemporal land cover mapping methodology, (ii) apply the methodology to create a time series of Canada from 1985 to 2000, and (iii) analyze the time series for general temporal and spatial trends.

The “Method” section of this paper gives an overview of the proposed multitemporal mapping approach. The section titled “Method implementation and product generation” provides particulars on the methodology, parameters used, data processing, and product generation for Canada, describes qualitative and quantitative evaluation procedures, and discusses limitations and possible improvements. In the “Time series analysis” section, an analysis of spatial and temporal patterns of disturbances demonstrates the use of the generated multiyear land cover database.

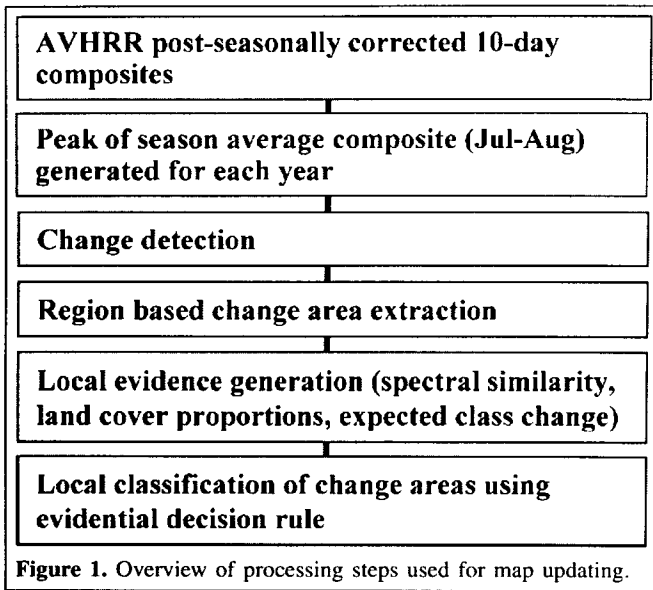
Method

Method overview

The multiyear land cover mapping procedure was designed specifically to maintain high consistency between land cover maps created on separate dates. For this, an existing map is updated to another year rather than creating completely new classifications for each year. The approach uses (i) change detection to identify areas that require updating and (ii) a local classification decision rule to determine the class for a pixel to be updated. **Figure 1** provides an overview of the processing steps involved in the updating procedure. A more detailed description of each step is provided in the following sections.

Change detection

The change detection technique uses a change vector approach to combine complementary information sources into a single indicator of change (IC). This indicator is based on the Euclidean distance between spectral bands and their texture



transforms scaled to a common range. IC is calculated to represent the change magnitude as follows:

$$IC = \sqrt{\sum_{i=1}^n (x_{it} - x_{it+\Delta t})^2} \quad (1)$$

where x_{it} is the pixel value for band i at time t , and $x_{it+\Delta t}$ is the value for the same band at time $t + \Delta t$.

Thresholds used for extracting change should be locally specified such that local influences (e.g., land cover type) on the change magnitude do not cause substantial error in change extraction. Ideally, training samples from an independent data source are needed to determine thresholds. In the absence of such data, visual comparison can be used, but with an associated increase in the subjectivity of the map production.

Local classification

The decision rule applied in the local classification uses information around a change object extracted as measures of evidence. For this application, these evidential measures include (i) local spectral signature evidence (LSSE), (ii) local class proportion evidence (LCPE), and (iii) expected class change evidence (ECCE) based on the previous pixel class and change direction.

Local spectral signature evidence

Local spectral signature evidence is a measure of the local spectral similarity between a pixel and each class within a specified sampling window. Spectral similarity is defined as the Euclidean distance between a change pixel to be classified and classes present in the sampling window using Equation (2). The Euclidean distance values are inverted so that larger values represent distances closer to a given class vector and normalized to sum to one:

$$LSSE_j = \frac{1}{\sqrt{\sum_{i=1}^n (x_i - m_{ij})^2}} \quad (2)$$

where x_i is the pixel value for band i , and m_{ij} is the mean value for band i and class j .

Two competing objectives are considered for defining the parameters used to control the size of the sample window: (i) generating signatures that effectively capture local spectral properties, and (ii) ensuring that all plausible signatures are included in the signature set for the local classification. The size of the window controls how well these criteria are met. Creating larger windows reduces the advantage gained by local processing (i.e., class signatures that are highly representative of the image area being classified), whereas small windows are sensitive to high-frequency noise and are more likely to exclude important land cover types from the classification decision. Generally, it is considered better to specify larger windows, as they are less susceptible to noise and are more likely to have all land cover types well represented.

Within the local window, signatures are generated using land cover data from the base land cover map with change areas removed. In generating LSSE of a class considered highly transient over the time period of interest, an option is provided to use a set of global signatures that can be inserted into the local signature set as a possible class for every change object. For example, classes representing disturbance should use globally defined signatures because the base map used for signature training will bias the signatures due to increased levels of vegetation found in these areas farther back or ahead in time.

Local class proportion evidence

Local class proportions are used to aid the classification decision when the surrounding landscape is considered to have some influence on the pixel being classified. For example, in backward updating an area to $t - \Delta t$, there is a greater likelihood that the land cover class of the area is that which surrounds it because of similar environmental factors (temperature, precipitation, soil, and topographic position) that are known to influence land cover distribution. This is also the case for forward updating $t + \Delta t$, as a given class is more likely to be developing towards the most frequently occurring land cover class around the change area for the same environmental factors and because the surrounding vegetation in this case is a potential seed source for recruitment post-disturbance. To include a measure of the local land cover proportion in the classification decision, the land cover proportions within a given distance of the change boundary are extracted and divided by the total area in this buffer.

Expected class change evidence

Two useful sources of information unique to this map-updating methodology include the change direction and the reference class value. With this information, constraints can be

developed to limit the classification decision to the most likely class value and remove or reduce the potential for highly unlikely classes to be considered. For example, a pixel classified as a recent burn at time t should not be classified as high-density conifer forest at time $t + \Delta t$ ($\Delta t = 5$). The time span of 5 years is not sufficient to allow for mature conifer redevelopment. This type of knowledge can be extremely useful in constraining the classification process. To utilize this information in the classification decision, expected change weight matrices were created for the time periods $t - \Delta t$ and $t + \Delta t$ and separately for positive and negative changes. Weights were assigned to reflect the expected changes that would most likely occur depending on the change direction and reference class value. The values in the weight matrices were normalized by dividing each individual weight by the sum of the weights for a given class value.

Evidence-based classification decision rule

To classify a pixel, three different rules were considered. **Figure 2** shows a flow diagram that summarizes the criteria used to determine which rule to apply.

The first rule was designed to ensure that a pixel was correctly identified as change and that it should be updated. For this, the maximum LSSE value is compared with the LSSE value associated with the reference classification label (i.e., class value for the map to be updated). If the difference between the maximum and the reference class LSSE value is less than a defined threshold, the pixel is not changed from its reference class.

The second rule is used to assign a pixel to a class in which the LSSE measure provides strong support. It recognizes that LSSE in this case can be used as the single information source in the classification decision.

If neither of the conditions for the first two rules are met, then the LSSE, LCPE, and ECCE are used to calculate a final evidence measure. It is implemented using Dempster's rule of

combination to combine the three evidence sources into a single value representing the support for each land cover class. The updated pixel label is defined as the class with the maximum support. Descriptions of Dempster's rule of combination applied to spatial data are given in Moon (1990), Srinivasan and Richards (1990), Peddle (1995a; 1995b), and Comber et al. (2004). A unique advantage of this approach is that it explicitly accounts for uncertainty associated with the evidential measures.

The three evidential measures are combined (E_c) using orthogonal summation denoted as follows:

$$E_c = LSSE \oplus LCPE \oplus ECCE \tag{3}$$

where \oplus represents the combination calculated for two sources i and j and set of labels A as

$$m_c = K^{-1} \sum_{A_i \cap A_j = A_n} m_1(A_i) m_2(A_j) \tag{4}$$

$$K = 1 - \sum_{A_i \cap A_j = \phi} m_1(A_i) m_2(A_j) \tag{5}$$

In the implementation, m is the mass or evidence value assigned to a class for a given source. The set of evidence values is referred to as an evidential vector, which is multiplied by a user-defined uncertainty factor to reflect the confidence with which a given evidence source has on the final decision. In Equation (4), K can be considered a measure of the extent of conflict between the two sources, and ϕ is the mass assigned to the null set, i.e., sum of mass contributed to conflicting labels.

Method implementation and product generation

The methodology described in the previous section was used to prepare consistent coarse-resolution land cover time series for 1985–2000 over Canada at 5-year time increments. Further description of procedure implementation, data preprocessing, and product evaluation is provided in the following sections.

Expected annual land cover change in Canada

Sources of change in Canada include forest harvesting, urban development, transportation corridors, mining, agriculture expansion–contraction, storms, fire, flooding, and insect and disease damage. To develop some insight into the expected annual change, a simple estimate was derived based on reported change sources for forested areas and assumed levels of change for others. Based on the annual average area of fire (2 million ha/year) and harvesting (1 million ha/year) from the National Forestry Database Program (Canadian Council of Forest Ministers, 2004) and an assumed annual average for other change sources of 2 million ha/year, the total percent change in respect to Canada's landmass (~100 million ha) is ~0.5%/year. The area affected by defoliation was not included in this estimate because moderate defoliation is difficult to detect in

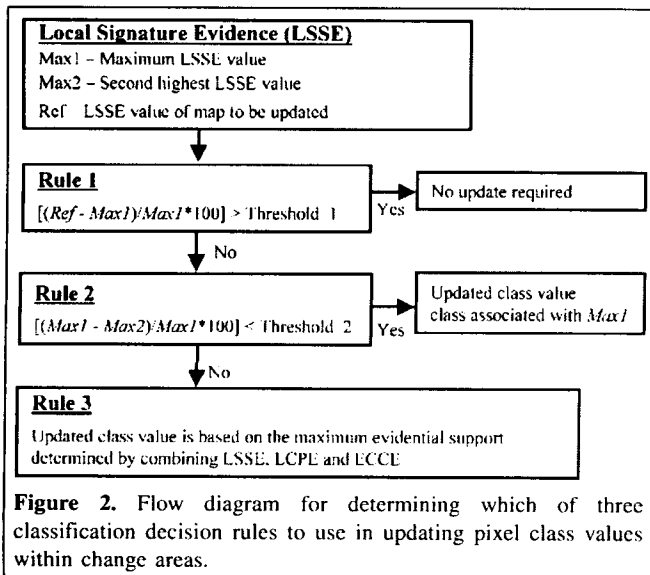


Figure 2. Flow diagram for determining which of three classification decision rules to use in updating pixel class values within change areas.

coarse-resolution imagery. Further, the reported area is inflated because the same area can be counted several times for each insect found to be impacting the area. It is important to note that the exact value was not required, just a reasonable estimate that could be used to guide selection of the updating interval and evaluate map consistency. Based on the annual change estimate over a 5-year period, cumulative change can be assumed to be approximately 3%. At this time interval, overall consistency of multitemporal land cover maps between time steps is expected to be greater than 90%, considering an assumed standard error of the 5-year change estimate of $\pm 5\%$.

Data and preprocessing

Satellite data

Satellite data acquired by AVHRR sensors NOAA 11 and 14 were used in this study because they were the only available data at the spatial and temporal resolution suitable for regional land cover mapping for the period of interest. Average images of red, near-infrared (Nir), and normalized difference vegetative index (NDVI) for the peak of the season (July 15 – August 15) and for each year (1985–2000) were created from 10-day post-seasonally corrected composites. The preprocessing prior to averaging included atmospheric correction, bidirectional reflectance normalization to a common viewing geometry, cloud screening, and seasonal profile interpolation following the methodology described in Cihlar et al. (2004). To improve multiyear data consistency, several normalization approaches based on robust regression were explored (Fernandes and Leblanc, 2005; Olthof et al., 2005). The normalization was applied to subsequent 10-day composites and average peak-of-season images. Normalization coefficients were derived following two sampling approaches: (i) sampling the whole image and (ii) ecozone-based stratified sampling. **Table 1** shows difference statistics for these modifications to the normalization procedure. Normalizing the 10-day composites improved results slightly over normalizing the peak-of-season average images. The ecozone-stratified normalization

produced the best results and thus was used as the normalization approach in this work.

Base map used for updating

The base map used for the updating procedure was the land cover map of Canada 1995 produced by Cihlar et al. (1999). This reference map was selected because it was produced using similarly processed AVHRR data available for this work and it is a widely accepted map product used by other Canadian government organizations. The map consists of the 31 classes summarized in **Table 2**.

Parameterization of change detection procedure

The coefficient of variation in a 5×5 pixel window was used as the texture transformation in the change detection procedure. This was considered a useful first-order texture measure that combines local variance and brightness into a single spatial discriminator. In calculating the change indicator (Equation (1)), the differences between bands were scaled to the range 0–1 for the spectral data and 0–0.5 for the texture data. This was done to normalize the weight of each input band. The reduced range for texture data was applied to moderate the influence of these bands in the change magnitude calculation.

To determine change thresholds, fire databases (Zhang et al., 2004a; 2004b; Fraser et al., 2004) and selected Landsat scenes were used. The fire databases covered the complete time period and were the main source of training data. Sources of Landsat data included a change database for the period 1998–2000 (Fraser et al., 2005), Landsat mosaic for 1990 available from the National Aeronautics and Space Administration (NASA; <http://www.esad.ssc.nasa.gov/>), and Landsat scenes for 2000 from the Center for Topographic Information (available from <http://geogratis.cgdi.gc.ca/>).

Almost all areas in the fire databases were identified by the change detection technique, but their areal extents were different. Thus, because the fire databases were constructed using more sophisticated procedures or coarse-resolution data

Table 1. Comparison of normalization methods based on robust regression using the 1995 composite as reference and 2000 as the composite to be corrected.

Method	Mean difference	Standard deviation difference	Mean absolute difference	Standard deviation absolute difference
Red band				
Peak-of-season composite (not normalized)	-4.47	33.52	15.30	30.15
Normalized peak-of-season composite	-1.15	30.82	14.63	27.14
Peak-of-season composite created from normalized 10-day composites	1.04	29.06	14.36	25.30
Ecozone-normalized peak-of-season composite	-0.01	25.26	14.03	21.00
Nir band				
Peak-of-season composite (not normalized)	17.92	30.21	24.89	24.78
Normalized peak-of-season composite	-0.24	30.80	17.12	25.60
Peak-of-season composite created from normalized 10-day composites	0.58	29.89	17.02	24.58
Ecozone-normalized peak-of-season composite	0.85	26.50	12.44	23.00

Note: All values are in digital numbers (DN).

Table 2. Summary of the 1995 31-class land cover legend, aggregate 12-class legend, and IGBP 16-class legend.

(A) 1995 31-class legend.		
Class	Label	
1	High density needleleaf forest	
2	Med density needleleaf forest	
3	Med density northern forest	
4	Low density southern forest	
5	Low density northern forest	
6	Deciduous forest	
7	Mixed needleleaf forest	
8	Mixed uniform forest	
9	Mixed heterogenous forest	
10	Mixed broadleaf forest	
11	New disturbance	
12	Old disturbance	
13	Transition tree shrubland	
14	Wetland tree shrubland	
15	Wetland medium density shrubs	
16	Grassland	
17	Lichen and other	
18	Shrub and lichen	
19	Heather and herbs	
20	Low vegetation cover nonforest	
21	Very low vegetation cover nonforest	
22	Barren	
23	Cropland high biomass	
24	Cropland med biomass	
25	Cropland low biomass	
26	Cropland-woodland	
27	Woodland-cropland	
28	Cropland-other	
29	Urban and built-up	
30	Water	
31	Snow/ice	
(B) 1995 12-class legend.		
Class	1995 31-class label	Label
1	1, 2, 3, 4	Conifer forest
2	6	Deciduous forest
3	7, 8, 9, 10	Mixed forest
4	11, 12	Disturbance
5	5, 13, 14, 15	Shrubland
6	16	Grassland
7	17, 18, 19, 20, 21, 22	Low vegetation and barren
8	23, 24, 25	Cropland
9	26, 27, 28	Cropland/woodland
10	29	Urban and built-up
11	30	Water
12	31	Snow/ice
(C) IGBP 16-class legend.		
Class	1995 31-class label	Label
1	1, 2, 3, 4	Evergreen needleleaf forest
2		Evergreen broadleaf forest
3		Deciduous needleleaf forest
4	6, 10	Deciduous broadleaf forest
5	7, 8, 9	Mixed forest
6	15	Closed shrublands
7	11, 12	Open shrublands

Table 2 (concluded).

(C) IGBP 16-class legend.		
Class	1995 31-class label	Label
8	5, 13	Woody savannas
9		Savannas
10	16	Grasslands
11	14	Permanent wetlands
12	23, 24, 25, 26, 27, 28	Croplands
13	29	Urban and built-up
14		Cropland/natural vegetation mosaic
15	31	Snow and ice
16	17, 18, 19, 20, 21, 22	Barren or sparsely vegetated

with higher spectral dimensions, burned areas from these databases for the change period were added to the change maps. A sieve filter was also applied to remove identified change areas less than 6 pixels in size considered to be mostly the result of noise. The direction of change required for the updating procedure was assigned to the change areas based on the difference in NDVI between the two dates. For forward updating, if NDVI was greater for the earlier date, then the pixel was assigned as negative change. If it was smaller for the earlier date, then it was assigned as positive change. This was reversed for backward updating.

Feature selection for classification procedure

To determine the best combination of data to be used for updating, a separability analysis (Bhattacharya; Richards, 1986) of the original 31 classes in the 1995 land cover map was conducted. Additional information and data transformations evaluated included surface temperature, texture, smoothing, and compositing period. Surface temperature was derived from AVHRR data and processed using the methods outlined in Cihlar et al. (2004). Texture data were derived using the coefficient of variation in the same manner as that used for change detection. Smoothing was applied using a 3×3 filter that did not include zero values in the average. Extreme values were also removed if they were two times larger than their surrounding nonzero neighbours. Three composites representing early season (11 and 21 April), mid-season (1, 11, and 21 July, 1 and 11 August), and late season (11 and 21 October) were generated for the red, Nir, and NDVI data from the 10-day AVHRR composite data. **Table 3** gives the average and minimum separability for the different data combinations examined. Overall, the separabilities were low, suggesting a reduced classification capability at the 31-class thematic level. The highest separability was obtained with the three composites periods for the red, Nir, and NDVI data. However, this data combination was not used for several reasons. First, data from the beginning and end of the growing season may be of reduced quality because measurements are strongly affected by clouds, haze, snow, and ice during these times. Second, several studies have shown that higher dimensionality may improve separability of training data, but often leads to overfitting and poor classification results (Jain et

Table 3. Bhattacharya separability measures for the different data combinations tested.

Data combination	Separability	
	Avg.	Min.
Red, Nir, NDVI	1.64	0.24
3×3 average filtered red, Nir, NDVI	1.70	0.30
Red, Nir, NDVI, RedTex	1.67	0.29
Red, Nir, NDVI, NirTex	1.66	0.25
Red, Nir, NDVI, NDVITex	1.67	0.28
Red, Nir, NDVI, SurfTemp	1.70	0.26
Early, mid, late season red composites	1.03	0.01
Early, mid, late season Nir composites	1.24	0.11
Early, mid, late season NDVI composites	1.21	0.03
Early, mid, late season red, Nir composites	1.65	0.32
Early, mid, late season red, Nir, NDVI composites	1.78	0.38

Note: Spectral composites are peak-of-season composites unless specified otherwise in the table.

al., 2000). Third, the improved separability was not considered to be of sufficient magnitude to warrant tripling the data input and processing load. For these reasons, the smoothed peak-of-season composite of red, Nir, and NDVI that produced the next highest separability was used for map updating.

Parameterization for local classification

The window size used for local classification was based on a visual assessment of the 1995 land cover distribution in Canada. It showed that window sizes of 400 km in the north-south direction and 800 km in the east-west direction should contain all locally suitable land cover classes while still being small enough to capture local spectral signature characteristics. The smaller value for the north-south direction was used to minimize the effects of more rapidly changing land cover in this direction.

Weight matrices were developed considering geographic and temporal development constraints. The weight matrices used in this implementation are shown in **Figure 3**. Each row of the matrices represents the evidence assigned to reflect the likelihood of the base map becoming one of the other map classes. The following were the most significant rules used in defining weights:

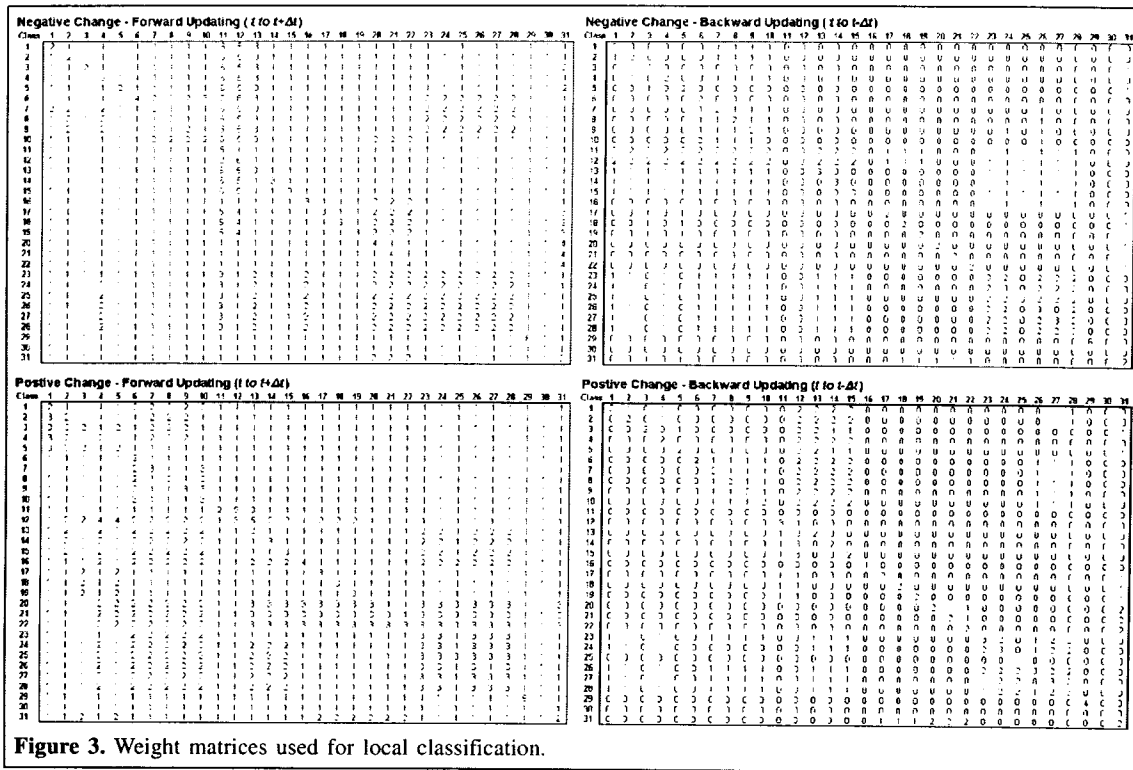


Figure 3. Weight matrices used for local classification.

- (1) Classes with a northern distribution (3, 5, 17–22, and 31) were likely to remain as one of these northern classes.
- (2) Classes with a southern distribution (1–2, 6–10, and 23–28) were likely to remain as one of these southern classes.
- (3) A high weight was assigned for a class in t to be the same class in $t + \Delta t$ or $t - \Delta t$.
- (4) For positive change, the following temporal trend was considered most likely for t to $t + \Delta t$ in forested areas: recent disturbance (class 11) → old disturbance (class 12) → shrub (classes 13–15) → forest (classes 1–10). For $t - \Delta t$, disturbance classes had a generally higher likelihood for conversion to forest and shrub classes.
- (5) For negative change, a class in t was assigned a high weight for conversion to recent and old disturbance at $t + \Delta t$ in forested areas. For $t - \Delta t$, forest and shrub classes had a higher weight for conversion to disturbance classes.

Thresholds used for determining which of the three classification rules (Figure 2) to apply were 5% for rule 1 and 25% for rule 2. The buffer around change areas used in extracting LCPE was set at 8 pixels. For evidential combination, the weights were set at 0.7 for LSSE, 0.4 for LCPE, and 0.8 for ECCE if the change direction was positive. If negative, the weight for LCPE was changed to 0.1, as the surrounding land cover was considered to have little influence on the classification decision in this situation. The high weight

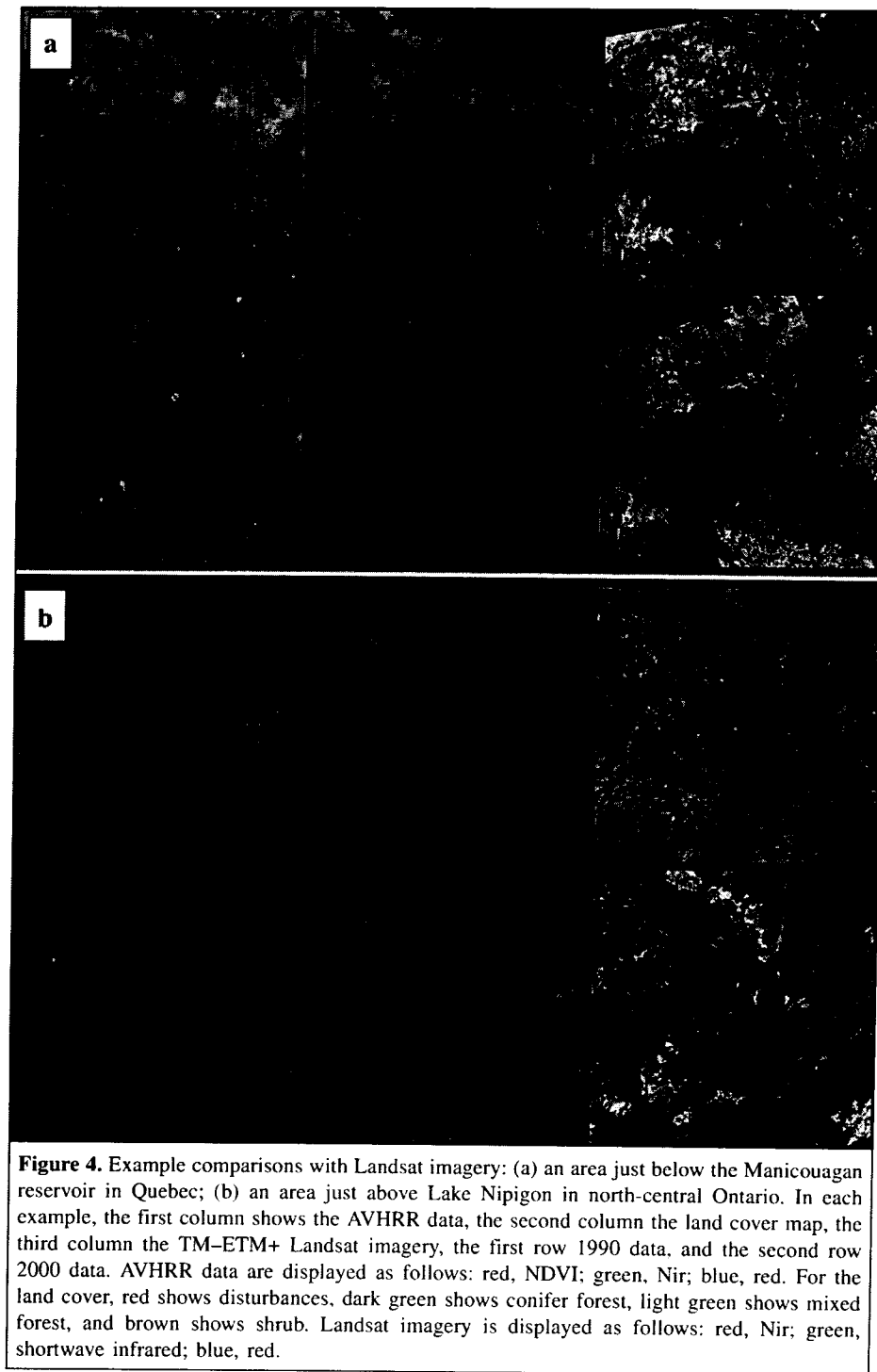
given to ECCE was used because LSSE provides little discrimination between classes in this case and therefore it is of reduced reliability. These parameters were empirically determined by processing sample areas taken from eastern, central, and northwestern Canada and comparing the results with the available reference data.

Product evaluation

The derived 1985–2000 land cover time series contains four maps of Canada at several levels of thematic detail based on three land cover legends: (i) 31-class land cover legend; (ii) aggregated versions to 12 classes, representing the collapsed hierarchy of the 31-class legend; and (iii) 16 classes based on the IGBP scheme (Table 2).

Qualitative evaluation

The generated land cover time series was visually assessed following a comparison with available fine-resolution reference data based on the procedure suggested by Mayaux (2002). Figure 4 shows two example areas from this assessment. Larger disturbances in both examples are detected, but their spatial shape and extent differ considerably from those of the Landsat imagery. Comparison of the lakes in the AVHRR and Landsat data shows that much of this difference is due to the spatial resolution capabilities of AVHRR. Small disturbances tend to be more frequently missed, such as the harvested areas in the lower section of Figure 4b. In this case, the change detection procedure often detected these disturbances, but only



a few pixels were identified and were later removed by the sieve filter.

The map products were also examined for the generally expected trend of forest disturbance and reestablishment. If the updating was correct, then the land cover changes should follow a logical temporal trajectory. Such an examination is demonstrated in **Figure 5**, which shows two sample areas of the

classified images from 1985–2000. The examples support the expected trend of forest disturbance and regrowth. The results are also spatially convincing, having relatively homogenous clusters created in change areas that blend well into their surroundings. The first example (**Figure 5a**) shows areas that were disturbed and are, or have, redeveloped to their predisturbance state. The second example (**Figure 5b**) depicts

an area of overall reduction of coniferous and mixed forest from 1985 to 2000.

Quantitative evaluation

Consistency assessment

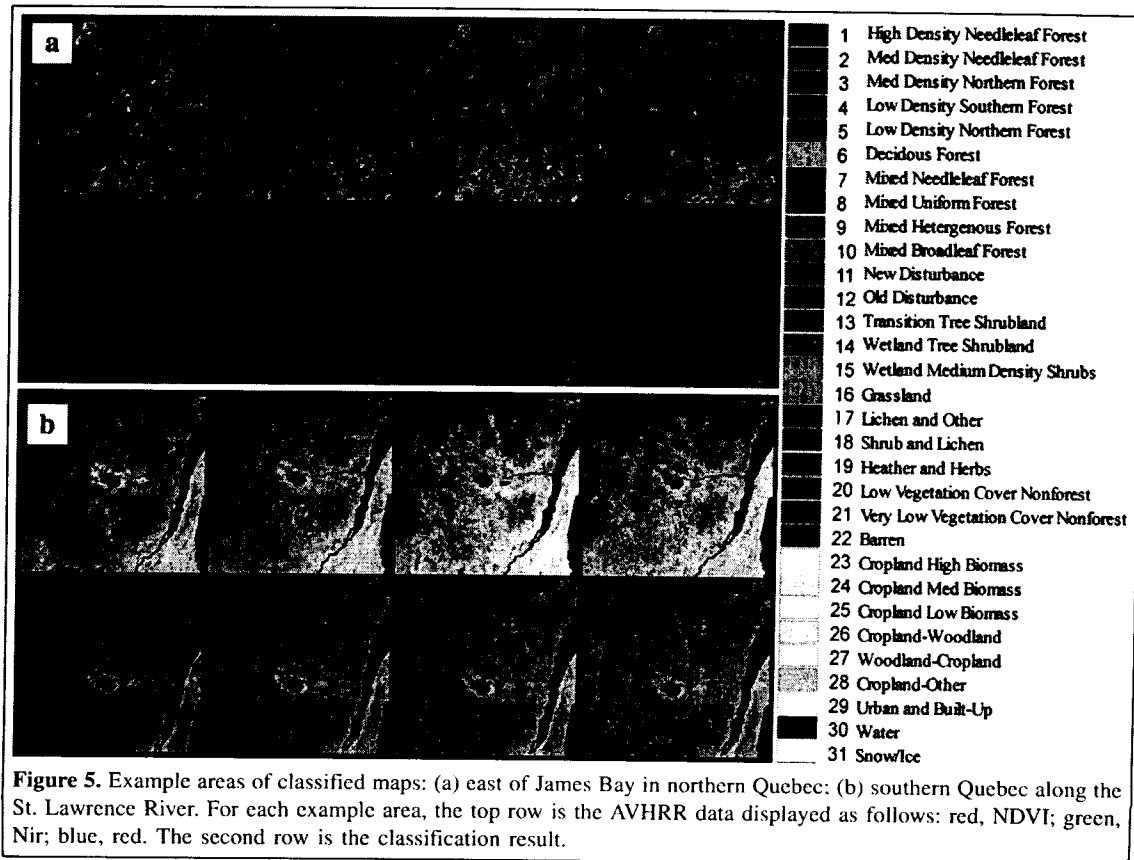
Consistency among the four maps is above the 90% expected for change areas in Canada over a 5-year period. Overall agreement for the 31-class legend was 96.1% for 1985–1990, 93.5% for 1985–1995, and 92.3% for 1985–2000. For the 12-class legend this same trend is seen with higher consistency, as agreements become more likely with fewer classes. Overall agreement for the 12-class legend was 97.3% for 1985–1990, 95.3% for 1985–1995, and 94.2% for 1985–2000. The lower rate of change in consistency with the longer time intervals is due to classes redeveloping towards their original predisturbance state over time.

Medium-resolution accuracy assessment

Quantitative accuracy assessment of multitemporal land cover products is difficult because of the lack of available reference data and the cost of developing a suitable database that could be used for validation of each time step. Fortunately, a medium-resolution database for 2000 was developed previously that could be used to assess and validate various aspects of the presented methodology. The Satellite Database for the Land Cover of Canada (SILC) is a 30 m resolution land

cover database consisting of 33 classified Landsat thematic mapper (TM) – enhanced thematic mapper plus (ETM+) scenes (Latifovic et al., 2002). Total sample size is 9% of the Canadian landmass. Scenes were selected using the purposive selection algorithm (Cihlar et al., 2000) to obtain a subset of scenes that represent the distribution of land cover across Canada. Classification was carried out following the enhancement classification method (Beaubien et al., 1999), with 46 land cover classes based on a modified National Vegetation Classification System (NVSC) Federal Geographic Data Committee (FGDC) classification system. Accuracy evaluation at a thematic resolution of 28 classes for 10 of the 33 scenes showed the overall accuracy to be 90.3% (Beaubien et al., 2001). For comparison with the land cover products in this study, the SILC data were resampled to 1 km pixel resolution, and the dominant land cover type within the 1 km pixel footprint was taken as the pixel label. The relative proportion of the dominant land cover type was also determined and used to create a second reference image representing the dominant fraction percent. To facilitate the direct comparison of the multitemporal land cover maps with SILC, the SILC legend was converted to the 31-class legend of the 1995 land cover map and the 16-class legend of the IGBP (Table 4).

The four maps were compared with the SILC database using three different legends (Table 2) and different ways of representing the SILC data. Comparisons included the dominant pixel fraction and dominant pixel fraction above 60%



for the entire SILC database and the areas identified as change. The different fraction thresholds were used for evaluating the method-labeling accuracy of homogenous pixels. Comparison for just change areas was also included so that the accuracy of the updating methodology could be more effectively evaluated.

Comparison using the entire SILC database showed that the best overall accuracy of 61.5% was achieved with the 12-class legend (Table 5). This was considerably higher than the accuracies obtained with the other legends and reveals the important dependence of accuracy on thematic resolution. The low accuracy found with the 31-class legend was expected because of a large number of mixed pixels with low homogeneity and considerable overlap of class spectral properties. For pixels with a dominant fraction greater than 60%, accuracies were much higher (47.3%–74.5%) depending on the legend used. Only slight differences were found between accuracies produced for the different years. In this case, using the entire SILC database tended to mask the effects of the improvement made by the updating procedure because the change areas only represent a small proportion of the SILC database. This combined with look-up table error for converting the FGDC legend to the 1995 legend were the main factors for the slight differences seen between the comparisons for the different years.

The results considering only the change areas showed that the 2000 map was in greater agreement than other land cover maps with the SILC database. This was expected because the SILC data were collected between 1998 and 2000. Overall accuracies in 2000 compared with 1995 increased by 6.8% for the 31-class legend and 7.8% for the 12-class legend. This increase was even more pronounced (ranging from 12.6% to 14.4%) when only pixels with a dominant fraction above 60% were included.

To identify the improvement gained by using local instead of global signatures, a simple Euclidean distance classification was performed using both methods of signature generation and compared with the SILC database. For the 31-class legend, overall accuracies in the change areas were 19.3% using local signatures and 18.0% using global signatures. For the 12-class legend, overall accuracies were 47.1% and 44.7% for local and global signatures, respectively, showing that local signatures increased the accuracy by 2.5%. The results here also provide insight into the improvement gained by the evidence-based classification, which was an increase of 16.8% over the simple Euclidean distance classification using global signatures.

It was also of interest to determine how well commission errors from the change detection procedure were corrected by the local classification methodology. For this assessment, 500 randomly located change objects of random size (5–200 pixels) were selected in areas identified as no-change in the 1995–2000 change map. These “false” changes were then classified using the local classification methodology with the 2000 AVHRR data and the overall accuracy calculated using the original 1995 land cover map for these false change areas. Results showed that reclassification accuracy was 41% for the 31-class legend and 72% for the 12-class legend.

Comparison using the IGBP legend is of interest because it allows for evaluation of the map accuracy relative to other maps of the region produced through global mapping initiatives. In Latifovic and Olthof (2004), the same SILC database and dominant fraction assessment procedure as that used here showed that the range of accuracies observed for four different global land cover products within Canada was 29%–49%. In this study, the 2000 land cover product achieved a higher accuracy estimate (52%), suggesting that it is possibly a better representation of Canada than the global products. In this case, the global mapping objective reduces the flexibility with which the map can be created to capture local variability, which can be more easily accounted for in regional-level mapping applications. Likely the most important factor is that a direct one-to-one merge of the different map legends was not possible due to overlap in class definitions leading to some degree of inherent error.

Limitations of medium-resolution accuracy assessment

The sampling objective used in the construction of the SILC database was to capture the land cover variability within Canada with the fewest possible scenes to minimize costs. Thus, the Landsat scenes in the database were distributed most frequently in areas of high land cover variability such as mountainous areas of British Columbia and transition zones between broad biomes. These areas are typically the most difficult to classify because of a greater occurrence of mixed pixels or topographic effects, and they only represent a small portion of the Canadian landmass. Complete random sampling would be more desirable so that sampling reflects the area distribution of land cover. The analysis within the change areas was the most influenced by the SILC sampling objective. For the analysis considering only change areas, the sample size was drastically reduced (only 6.8% of the SILC area), making the results more sensitive to errors in either the SILC database, 2000 land cover, or change detection inputs. The SILC sample scenes also miss the majority of the high temporal and spatial change areas and are most prevalent in areas where change accuracy is expected to be the lowest, such as areas with strong topography leading to high proportions of false change detection.

Another limitation of this validation is the effect of the conversion table used to merge the 46-class FGDC legend used in SILC with the 31-class legend. Some of the SILC database classes do not clearly associate with a single class in the 31-class legend. Thus, changes in how classes are merged can have a substantial impact on accuracy assessment. In the SILC database, for example, numerous old burns are labeled as low vegetation cover, whereas in the land cover time series these areas are labeled as old disturbance, resulting in error. Unfortunately, changing either class in an attempt to improve agreement results in similar or greater error.

Table 4. Look-up table for converting the SILC legend to the 16-class IGBP legend and 1995 31-class legend.

Federal Geographic Data Committee (FGDC) classification		16-class IGBP	1995 31-class
Tree dominated (tree crown density > 25%)			
1	Evergreen forest (>75% cover) — old	1	1
2	Evergreen forest (>75% cover) — young	1	4
3	Deciduous forest (>75% cover)	4	10
4	Mixed coniferous (50%–75% coniferous) — old	5	9
5	Mixed coniferous (50%–75% coniferous) — young	5	9
6	Mixed deciduous (25%–50% coniferous)	5	9
7	Evergreen open canopy (40%–60% cover) — moss–shrub understory	1	1
8	Evergreen open canopy (40%–60% cover) — lichen–shrub understory	1	2
9	Evergreen open canopy (25%–40% cover) — shrub–moss understory	1	4
10	Evergreen open canopy (25%–40% cover) — lichen (rock) understory	1	5
11	Deciduous open canopy (25%–60% cover)	4	10
12	Deciduous open canopy — low regenerating to young broadleaf cover	4	10
13	Mixed evergreen–deciduous open canopy (25%–60% cover)	5	9
14	Mixed deciduous (25%–50% coniferous trees; 25%–60% cover)	5	9
15	Low regenerating to young mixed cover	5	9
Shrub dominated			
16	Deciduous shrubland (>75% cover)	6	14
Herb dominated			
17	Grassland, prairie region	10	16
18	Herb – shrub – bare cover, mostly after perturbations	7	5
19	Shrubs–herb–lichen–bare	7	19
20	Wetlands	11	14
21	Sparse coniferous (density 10%–25%), shrub–herb–lichen cover	8	5
22	Sparse coniferous (density 10%–25%), herb–shrub cover	8	13
23	Herb–shrub	16	18
24	Shrub–herb–lichen–bare	16	18
25	Shrub – herb – lichen – water bodies	16	18
26	Lichen–shrub–herb, bare soil or rock outcrop	16	17
27	Lichens–shrub–herb, bare soil – rock outcrop, water bodies	16	17
28	Low vegetation cover (bare soil, rock outcrop)	16	21
29	Low vegetation cover, with snow	16	20
30	Woodland–cropland	0	27
31	Cropland–woodland	0	26
32	Annual row-crop forbs and grasses — high biomass	12	23
33	Annual row-crop forbs and grasses — medium biomass	12	24
34	Annual row-crop forbs and grasses — low biomass	12	25
Nonvascular dominated			
35	Lichen barren	16	18
36	Lichen–shrub–herb–bare	16	19
37	Sparse coniferous (density 10%–25%), lichen–shrub–herb cover	16	13
Vegetation not dominant			
38	Rock outcrop, low vegetation cover	16	21
39	Recent burns	7	11
40	Mostly bare disturbed areas (e.g., cutovers)	7	11
41	Low vegetation cover	16	12
42	Urban and built-up	13	29
43	Water bodies	0	0
44	Mixes of water and land	0	0
45	Snow/ice	15	31
46	Clouds	0	0

Table 5. Overall and kappa accuracy measures for various comparisons with the SILC database.

	1985		1990		1995		2000	
	Overall	Kappa	Overall	Kappa	Overall	Kappa	Overall	Kappa
31-class land cover comparison with SILC database								
SILC	27.10	0.255	27.18	0.256	27.12	0.253	27.73	0.260
SILC dominant fraction > 60%	46.10	0.431	46.09	0.431	45.95	0.427	47.30	0.440
SILC change areas only	18.82	0.170	18.40	0.152	17.16	0.138	23.94	0.216
SILC change areas only dominant fraction > 60%	27.79	0.266	26.03	0.237	23.23	0.208	35.85	0.350
16-class IGBP land cover comparison with SILC database								
SILC	51.69	0.466	51.63	0.477	51.80	0.476	52.06	0.470
SILC dominant fraction > 60%	66.15	0.609	66.80	0.617	66.23	0.610	66.88	0.618
SILC change areas only	34.73	0.290	36.08	0.310	34.37	0.281	37.33	0.321
SILC change areas only dominant fraction > 60%	30.42	0.227	31.85	0.245	31.15	0.241	41.05	0.354
12-class land cover comparison with SILC database								
SILC	60.46	0.552	60.73	0.555	60.72	0.555	61.50	0.564
SILC dominant fraction > 60%	72.69	0.667	72.60	0.666	72.60	0.666	74.05	0.684
SILC change areas only	36.46	0.247	36.25	0.205	36.31	0.235	43.97	0.301
SILC change areas only dominant fraction > 60%	42.45	0.298	39.35	0.242	42.02	0.343	56.35	0.439

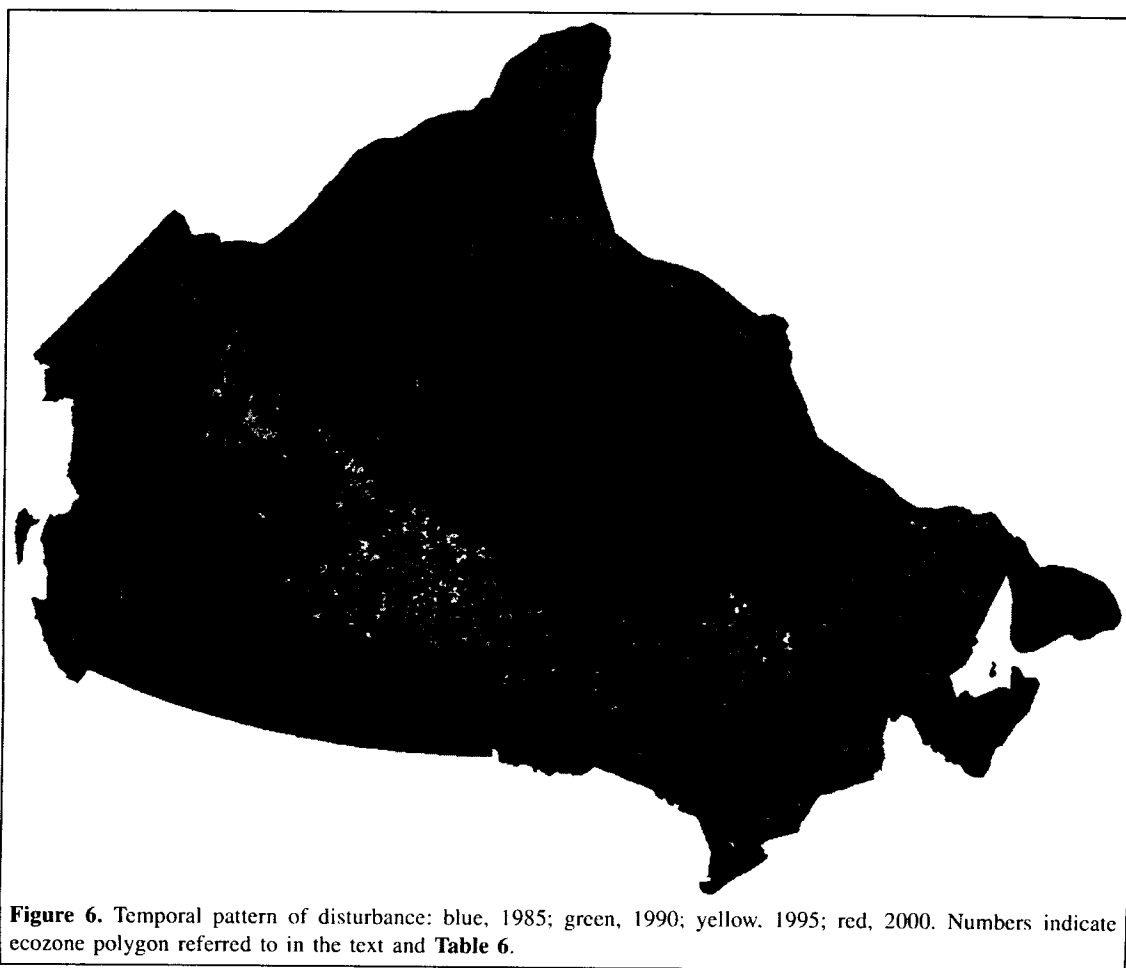


Table 6. Percent land cover area to the total ecozone area for selected ecozones.

Ecozone	Year	Land cover class					
		Conifer forest (1)	Deciduous forest (2)	Mixed forest (3)	Disturbance (4)	Shrubland (5)	Grassland (6)
Taiga Shield West (5)	1985	57.15	0.00	0.06	4.16	9.92	0.00
	1990	54.08	0.00	0.07	6.21	10.16	0.00
	1995	46.76	0.00	0.07	13.65	10.22	0.00
	2000	46.39	0.00	0.07	14.26	10.17	0.00
Boreal Shield East (6)	1985	39.21	1.25	41.18	0.41	14.05	0.00
	1990	39.29	1.15	42.08	0.33	13.17	0.00
	1995	38.79	1.35	41.80	0.69	13.32	0.00
	2000	37.35	1.35	41.80	2.05	13.44	0.00
Prairies (10)	1985	0.02	0.00	0.85	0.00	0.91	10.35
	1990	0.02	0.00	0.85	0.00	0.91	10.39
	1995	0.02	0.00	0.85	0.00	0.91	10.39
	2000	0.02	0.00	0.85	0.00	0.91	10.38
Boreal Cordillera (12)	1985	41.81	0.04	4.51	0.81	30.15	0.00
	1990	40.89	0.04	4.26	1.26	30.48	0.00
	1995	40.19	0.04	4.31	1.67	30.49	0.00
	2000	40.37	0.04	4.26	1.65	30.45	0.00
Taiga Shield East (16)	1985	43.50	0.00	0.02	1.33	8.09	0.00
	1990	40.55	0.00	0.03	3.97	8.25	0.00
	1995	39.19	0.00	0.03	5.14	8.31	0.00
	2000	41.43	0.00	0.03	3.26	8.23	0.00
Boreal Shield West (17)	1985	80.95	0.00	9.50	2.87	5.77	0.00
	1990	76.63	0.00	9.55	6.68	6.05	0.00
	1995	74.27	0.00	9.95	9.13	5.58	0.00
	2000	75.80	0.00	9.79	6.47	6.91	0.00
Canada	1985	30.91	0.40	12.88	0.88	10.99	0.55
	1990	30.06	0.38	12.99	1.60	10.89	0.56
	1995	28.99	0.40	12.89	2.68	10.92	0.56
	2000	29.12	0.40	12.87	2.55	10.99	0.56

Note: Class and ecozone numbers are given in parentheses.

Factors affecting land cover database consistency and potential improvements

An account of the potential error sources in the methodology is useful to identify areas of improvement and to better educate users on the potential limitations that may translate to map uncertainty. The error sources include AVHRR data, change detection, the base map used for updating, and local classification. The methods used for preprocessing the AVHRR data have been well established and validated. However, there is potential for improvements and advancements in data processing, which are continually being explored.

Change detection offers some potential for improvement, as reclassification of false change areas was 76% for the 12-class legend. However, considering that false change is only a small portion of the total change area and that the majority of this error will be correctly reclassified reduces the sensitivity of the method to commission error. Regardless, improvements made will benefit the final product accuracy. More advanced change detection techniques or fusion of change methods could lead to improved results. The main difficulty with change detection is the selection of appropriate change indicators and thresholds. The simplest way to achieve this is with improved training data.

The accuracy of the base map is important because it is used for signature generation and to constrain the classification using the expected class change weight matrix. Thus, an accurate base map is an important factor. Unfortunately, there is little that can be done to improve the map once it is selected or produced without recreating the classification using an improved methodology or data.

More rigorous development of the weight matrices used to represent expected class changes could be developed. The weight matrix significantly constrains the classification, and the more effectively this matrix is specified, the more accurate the time series developed will be. Ideally, a group of experts should be assembled to give input for the development of the weight matrix. However, this will depend on the availability of such expertise.

Time series analysis

The multiyear land cover database supports a generally accepted conclusion that a land cover product should be based on earth observation rather than survey map compilation, and that a database spatial resolution of 1 km is currently appropriate for meeting the wide range of emerging global and

Low vegetation (7)	Cropland (8)	Cropland-woodland (9)	Urban (10)	Snow-ice (12)
28.69	0.00	0.02	0.00	0.00
29.46	0.00	0.02	0.00	0.00
29.27	0.00	0.02	0.00	0.00
29.09	0.00	0.01	0.00	0.00
2.98	0.10	0.70	0.11	0.00
3.02	0.11	0.73	0.11	0.00
3.08	0.12	0.73	0.11	0.00
3.04	0.13	0.73	0.11	0.00
0.02	66.94	20.51	0.40	0.00
0.02	66.97	20.44	0.40	0.00
0.02	66.97	20.44	0.40	0.00
0.02	66.98	20.44	0.40	0.00
20.82	0.00	0.00	0.00	1.85
20.93	0.00	0.00	0.00	2.14
21.63	0.00	0.00	0.00	1.66
20.94	0.00	0.00	0.00	2.29
47.06	0.00	0.00	0.00	0.01
47.19	0.00	0.00	0.00	0.01
47.32	0.00	0.00	0.00	0.00
47.05	0.00	0.00	0.00	0.00
0.64	0.03	0.19	0.02	0.03
0.78	0.07	0.19	0.02	0.03
0.75	0.07	0.18	0.02	0.04
0.72	0.08	0.17	0.02	0.03
27.97	4.74	2.79	0.11	7.77
28.15	4.80	2.73	0.11	7.73
28.28	4.82	2.72	0.11	7.63
28.11	4.81	2.72	0.11	7.75

regional modeling applications (Loveland et al., 2000). The methodology for generating the land cover time series was employed at the 31-class level because it is the highest thematic level available for the 1995 land cover base map. This allows for numerous aggregate legends to be devised for various analysis tasks of interest. It also allows for tracking a single well-defined class through time with an associated level of uncertainty. The exact thematic resolution and legend used will depend on the objectives of the analyst balancing the objective with the allowable uncertainty. To recognize the range of applications in which the multiyear land cover database can provide information, an example is presented of analyzing spatial and temporal patterns and their variations for the period 1985–2000 over the Canadian landmass.

An analysis of class area can be performed using different thematic resolutions and stratification schemes. The land cover composition for 17 Canadian ecozones as defined by the Ecological Stratification Working Group (Marshall and Schut, 1999) was used in this study. The analysis was performed using the legend with 12 major land cover types. **Figure 6** shows the spatial distribution of disturbance through time and readily depicts areas with extensive spatial and high temporal disturbance. The size distribution of disturbance is also evident,

with the majority of large disturbances occurring in ecozones 4 and 5 and the northern portion of ecozone 17. These disturbances are predominately the result of fire, but other causes include harvesting, mining, and severe insect defoliation. In the southern portion of ecozone 17 the smaller sized disturbances are mostly due to forest harvesting. In the far north (ecozones 1–3), little land cover disturbance has been identified, as the annual spatial dynamics and surface variability of snow and ice make it difficult to determine significant land cover change in these areas. The combined effects of annual snow and ice and topography also reduce detection capabilities in western British Columbia. In the prairie ecozone (ecozone 10), annual fluctuations in moisture can lead to dramatically different appearance of surface types, making disturbance more difficult to detect. Davidson and Wang (2004) found that the shortwave surface albedo of grasslands was almost two times more variable than that of forest cover types.

Table 6 presents results of the percent class area to total ecozone area for selected ecozones from 1985 to 2000. As with **Figure 6**, this table highlights ecozones with highly variable and stable land cover distribution through time. Ecozones 5, 16, and 17 have the most significant forest cover change for the 20-year period analyzed. The changes in ecozones 5, 16, and 17 contribute to a reduction in the total forest area of 2.1%, 1.4%, and 4.4% respectively. Following the forest area through time shows the majority of the disturbance for ecozones 16 and 17 occurred in the period 1985–1990, but the majority of disturbance for ecozone 5 occurred in the period 1990–1995. Examination of change for all of Canada shows an overall reduction of coniferous forest area from 1985 to 2000. This is in part due to high fire incidence years occurring in 1989 and 1995 and due to a limited ability to backward update disturbed areas. The difficulty is that the unique spectral response of disturbance changes quickly to appear similar to that of other land cover classes within a few years depending on location. In the north, vegetation redevelopment is slower and thus the disturbance signal is maintained for a longer time, whereas in the south the disturbance signal can dissipate much more rapidly (Zhang et al., 2004b). In forward updating, knowledge of post-disturbance succession captured in the ECCE reduces this problem. In backward updating, however, this knowledge cannot be applied in the same manner, resulting in underestimation of disturbance. In 2000, the loss of forest is beginning to be offset by regeneration of 1985–1990 disturbed areas. No significant change in the cropland class with regards to an increase or decrease in area is seen, which is consistent with census data (Statistics Canada, 2001). However, the land cover products underestimate the total area by 2% for the combined cropland and cropland-woodland classes. The difference is mostly due to the inability of detecting cropland areas less than 1 km² with coarse-resolution satellite imagery. All other land covers appear to be relatively stable over the time period examined.

Conclusion

In this research, a new map-updating methodology was developed and used to create a land cover time series over Canada for the period 1985–2000. The multiyear data follow logical temporal and spatial trends in land cover and were highly consistent between years, with overall agreement greater than 92%. Comparison with a medium-resolution reference database showed the map accuracy to be 61% at a thematic resolution of 12 classes, and it had an accuracy similar to that of other global land cover products. It also showed that the methodology considerably improved the accuracy of areas identified as change as the date of the land cover map came closer to the date of the validation database (SILC, increase of 8%). These maps could be used in a variety of ways to assess land cover changes through time and as inputs to regional-level ecosystem process models. Further development of the methodology and modifications of products will be considered as errors are identified through more detailed accuracy evaluations.

Acknowledgements

This research has been completed as a part of the Natural Resources Canada Earth Sciences Sector program Reducing Canada's Vulnerability to Climate Change, partially supported by the Canadian Space Agency funded project Climate Change and Ecosystem Impact. We would like to thank Goran Pavlic and Robert Fraser for providing the fire and Landsat change databases used in the study. We would also like to thank Gunar Fedosejevs and Bert Guindon for their valuable reviews of this manuscript and two anonymous reviewers.

References

- Beaubien, J., Cihlar, J., Simard, G., and Latifovic, R. 1999. Land cover from multiple thematic mapper scenes using a new enhancement-classification methodology. *Journal of Geophysical Research*, Vol. 104, pp. 27 909 – 27 920.
- Beaubien, J., Latifovic, R., Cihlar, J., and Simard, G. 2001. *BOREAS follow-on DSP-01 Landsat TM land cover mosaic of the BOREAS transect*. Oak Ridge National Laboratory Distributed Active Archive Center, Oak Ridge, Tenn. Available from <http://www.daac.ornl.gov> [accessed 11 December 2004].
- Canadian Council of Forest Ministers. 2004. *National Forestry Database Program*. Available from <http://nfdp.ccfm.org> [accessed 10 September 2004].
- Cihlar, J., Beaubien, J., Latifovic, R., and Simard, G. 1999. *Land cover of Canada version 1.1*. CD-ROM. Natural Resources Canada, Ottawa, Ont.
- Cihlar, J., Latifovic, R., Chen, J., Beaubien, J., and Li, Z. 2000. Selecting representative high-resolution sample images for land cover studies: part 1 methodology. *Remote Sensing of Environment*, Vol. 71, pp. 26–42.
- Cihlar, J., Latifovic, R., Chen, J., Trishchenko, A., Du, Y., Fedosejevs, G., and Guindon, B. 2004. Systematic corrections of AVHRR image composites for temporal studies. *Remote Sensing of Environment*, Vol. 89, pp. 217–233.
- Comber, A.J., Law, A.N.R., and Lishman, J.R. 2004. A comparison of Bayes', Dempster-Shafer and Endorsement theories for managing knowledge uncertainty in the context of land cover monitoring. *Computers, Environment and Urban Systems*, Vol. 28, pp. 311–327.
- Coppin, P., and Bauer, M. 1996. Digital change detection in forest ecosystems with remote sensing imagery. *Remote Sensing Reviews*, Vol. 13, pp. 207–234.
- Coppin, P., Jonckheere, I., Nackaerts, K., Muys, B., and Lambin, E. 2004. Digital change detection methods in ecosystem monitoring: a review. *International Journal of Remote Sensing*, Vol. 25, No. 9, pp. 1565–1596.
- Davidson, A., and Wang, S. 2004. The effects of sampling resolution on the surface albedos of dominant land cover types in the North American boreal region. *Remote Sensing of Environment*, Vol. 93, pp. 211–224.
- DeFries, R., and Townshend, J. 1994. NDVI-derived land cover classification at global scales. *International Journal of Remote Sensing*, Vol. 15, pp. 3567–3586.
- Fernandes, R., and Leblanc, S. 2005. Appropriate linear regression techniques for the calibration of remote sensing models: when classical linear regression should not be used. *Remote Sensing of Environment*, Vol. 95, pp. 303–316.
- Footy, G. 2001. Monitoring the magnitude of land-cover change around the southern limits of the Sahara. *Photogrammetric Engineering and Remote Sensing*, Vol. 67, pp. 841–847.
- Fraser, R., Hall, R., Landry, R., Lynham, T., Raymond, D., Lee, B., and Li, Z. 2004. Validation and calibration of Canada-wide-resolution satellite burned area maps. *Photogrammetric Engineering and Remote Sensing*, Vol. 70, pp. 451–460.
- Fraser, R., Abuelgasim, A., and Latifovic, R. 2005. A method for detecting large-scale forest cover change using coarse spatial resolution imagery. *Remote Sensing of Environment*, Vol. 30, pp. 414–427.
- Hall, F., Botkin, D., Strelbel, D., Woods, K., and Goetz, S. 1991. Large-scale patterns of forest succession as determined by remote sensing. *Ecology*, Vol. 72, pp. 628–640.
- Hansen, M., DeFries, R., Townshend, J., and Sohlberg, R. 2003. Global land cover classification at 1 km spatial resolution using a classification tree approach. *International Journal of Remote Sensing*, Vol. 21, pp. 1331–1364.
- Jain, A., Duin, R., and Mao, J. 2000. Statistical pattern recognition: a review. *IEEE Transactions on Pattern Analysis and Machine Intelligence*, Vol. 22, pp. 4–37.
- Jensen, J. 1996. *Introductory digital image processing: a remote sensing perspective*. Prentice-Hall Inc., Englewood Cliffs, N.J.
- Latifovic, R., and Olthof, I. 2004. Accuracy assessment using sub-pixel fractional error matrices of global land cover products derived from satellite data. *Remote Sensing of Environment*, Vol. 90, pp. 153–165.
- Latifovic, R., Beaubien, J., and Cihlar, J. 2002. *Land cover classification of Landsat ETM+ scene 26 July 1999 Path 09/Row 23. Satellite information for land cover of Canada (SILC) project*. Canada Centre for Remote Sensing, Natural Resources Canada, Ottawa, Ont.
- Latifovic, R., Zhu, Z., Cihlar, J., Giri, C., and Olthof, I. 2004. Land cover mapping of North and Central America — Global Land Cover 2000. *Remote Sensing of Environment*, Vol. 89, pp. 116–127.
- Latifovic, R., Fytas, K., Chen, J., and Paraszczak, J. 2005. Assessing land cover change resulting from large surface mining development.

- International Journal of Applied Earth Observation and Geoinformation*, Vol. 7, pp. 29–48.
- Loveland, T., and Belward, A. 1997. The IGBP-DIS global 1 km land cover data set, DISCover: first result. *International Journal of Remote Sensing*, Vol. 18, pp. 1389–3296.
- Loveland, T., Reed, B., Brown, J., Ohlen, D., Zhu, Z., Yang, L., and Merchant, J. 2000. Development of a global land cover characteristics database and IGBP DISCover from 1 km AVHRR data. *International Journal of Remote Sensing*, Vol. 21, pp. 1303–1330.
- Lu, D., Mausel, P., Brondizio, E., and Moran, E. 2004. Change detection techniques. *International Journal of Remote Sensing*, Vol. 25, pp. 2365–2407.
- Marshall, I., and Schut, P. 1999. *A national ecological framework for Canada*. A cooperative product by Ecosystems Science Directorate, Environment Canada, and Research Branch, Agriculture and Agri-Food Canada. Ottawa, Ont. Available from <http://sis.agr.gc.ca/cansis/nsdb/ecostrat/intro.html> [accessed 9 August 2004].
- Mas, J. 1999. Monitoring land-cover changes: a comparison of change detection techniques. *International Journal of Remote Sensing*, Vol. 20, pp. 139–152.
- Maxwell, S., Hoffer, R., and Chapman, P. 2002a. AVHRR composite period selection for land cover classification. *International Journal of Remote Sensing*, Vol. 23, pp. 5043–5059.
- Maxwell, S., Hoffer, R., and Chapman, P. 2002b. AVHRR channel selection for land cover classification. *International Journal of Remote Sensing*, Vol. 23, pp. 5061–5073.
- Mayaux, P. 2002. GLC 2000 project — guidelines for quality control. In *Proceedings of the GLC 2000 Meeting, Ispra, Italy, March 2002*. Available from <http://www-gvm.jrc.it/glc2000/publications.htm> [accessed 2 August 2004].
- Miller, A., Bryant, E., and Birnie, R. 1998. An analysis of land cover changes in the northern forest of New England using multitemporal Landsat MSS data. *International Journal of Remote Sensing*, Vol. 19, pp. 245–265.
- Moon, W. 1990. Integration of geophysical and geological data using evidential belief function. *IEEE Transactions on Geoscience and Remote Sensing*, Vol. 28, pp. 711–720.
- Olthof, I., Pouliot, D., Fernandes, R., and Latifovic, R. 2005. Landsat ETM+ radiometric normalization comparison for northern mapping applications. *Remote Sensing of Environment*, Vol. 95, pp. 388–398.
- Peddle, D. 1995a. Knowledge formulation for supervised evidential classification. *Photogrammetric Engineering and Remote Sensing*, Vol. 61, pp. 409–417.
- Peddle, D. 1995b. MERCURY[®]: an evidential reasoning image classifier. *Computers and Geosciences*, Vol. 21, pp. 1163–1176.
- Richards, J.A. 1986. *Remote sensing digital image analysis*. Springer-Verlag, New York.
- Srinivasan, A., and Richards, J. 1990. Knowledge-based techniques for multi-source classification. *International Journal of Remote Sensing*, Vol. 11, pp. 505–525.
- Statistics Canada. 2001. *2001 census of agriculture*. Available from <http://www.statcan.ca/english/agcensus2001/index.htm> [accessed 11 October 2004].
- Stöckli, R., and Vidale, P.L. 2004. European plant phenology and climate as seen in a 20-year AVHRR land-surface parameter dataset. *International Journal of Remote Sensing*, Vol. 25, pp. 3303–3330.
- Strahler, A., Muchoney, D., Borak, J., Friedl, M., Gopal, S., Lambin, E., and Moody, A. 1999. *MODIS land cover product algorithm theoretical basis document (ATBD), version 5.0*. NASA EOS_MTPE Documentation, NASA, Washington, D.C.
- Townshend, J., Justice, C., and Kalb, V. 1987. Characterization and classification of South American land cover types using satellite data. *International Journal of Remote Sensing*, Vol. 8, pp. 1189–1207.
- Trishchenko, A.P., Cihlar, J., and Li, Z. 2001. Effects of spectral response functions on surface reflectance and NDVI measured with moderate resolution satellite sensors. *Remote Sensing of Environment*, Vol. 81, pp. 1–18.
- Tucker, C., Townshend, J., and Goff, T. 1984. Continental land cover classification using meteorological satellite data. *Science (Washington, D.C.)*, Vol. 227, pp. 369–375.
- Zhang, Q., Pavlic, G., Chen, W., Fraser, R., Leblanc, S., and Cihlar, J. 2004a. A semi-automatic segmentation procedure for feature extraction in remotely sensed imagery. *Computers and Geosciences*, Vol. 31, pp. 289–296.
- Zhang, Q., Pavlic, G., Chen, W., Latifovic, R., Fraser, R., and Cihlar, J. 2004b. Deriving stand age distribution in boreal forests using SPOT/VEGETATION and NOAA AVHRR imagery. *Remote Sensing of Environment*, Vol. 91, pp. 405–418.